Front. Phys. 10, 102101 (2015)
DOI 10.1007/s11467-015-0474-0

RESEARCH ARTICLE

Shape coexistence and α-decay chains of ^{293}Lv

Zhao-Xi Li (李兆玺)[1], Zhen-Hua Zhang (张振华)[2,3], Peng-Wei Zhao (赵鹏巍)[2,†]

[1] *School of Physics and Nuclear Energy Engineering, Beihang University, Beijing 100191, China*
[2] *State Key Laboratory of Nuclear Physics and Technology, School of Physics, Peking University, Beijing 100871, China*
[3] *Mathematics and Physics Department, North China Electric Power University, Beijing 102206, China*

Corresponding author. E-mail: †pwzhao@pku.edu.cn

Received January 24, 2015; accepted March 10, 2015

Two recently observed ^{293}Lv ($Z = 116$) α-decay chains [*Eur. Phys. J. A* 48, 62 (2012)] are investigated in the framework of covariant density functional theory with PC-PK1, where the pairing correlations are treated by the Bardeen–Cooper–Schrieffer method with a density-independent zero-range force. From the calculated potential energy curves, it is found that two minima always occur, with one having an almost spherical shape and the other exhibiting a large deformed prolate shape. Originating from the ground state and the shape-isomeric state of ^{293}Lv, the two observed α-decay chains are constructed and the calculated Q_α values are found to be in good agreement with the data.

Keywords shape coexistence, α decay, ^{293}Lv, covariant density functional theory

PACS numbers 21.10.Dr, 21.60.Jz, 23.60.+e, 27.90.+b

Due to quantum shell effects, the existence of an island of stability in the region of the superheavy nuclei (SHN) at around $Z = 114$ and $N = 184$ was first predicted in the 1960's [1–8]. Since then, investigation of the properties of SHN has been a topic of considerable interest and also a significant challenge in nuclear physics. In experimental studies, which have benefited from the improvement of beam intensities and detection efficiencies, superheavy elements with $Z \leqslant 118$ have been synthesized via cold and/or hot fusion reactions [9–13]. Theoretically, a number of investigations (for reviews, see, e.g., Ref. [14]) have been devoted to the SHN structure, which were primarily based on either traditional macroscopic-microscopic or microscopic self-consistent approaches. In particular, self-consistent mean-field models based on nuclear energy density functionals [15] have been extensively applied to investigate the various properties of SHN, such as their ground-state properties [16–18], shell structures [19–22], α-decay energies and half-lives [23, 24], fission barriers [25–29], and shape transitions [30]. As regards nuclear reaction, the nucleosynthesis of SHN has been extensively investigated using the dinuclear system model [31–37], the fluctuation-dissipation model [38], the fusion-by-diffusion model [39–42], the quantum molecular dynamics model [43, 44], the two-step model [45], and other models [46, 47].

Focusing on Lv isotopes, $^{290-293}$Lv were first discovered at the Joint Institute for Nuclear Research Flerov Laboratory of Nuclear Reactions (JINR-FLNR) in Dubna (Russia) [48, 49]. For ^{293}Lv in particular, the decay properties were measured through the fusion-evaporation reaction, ^{248}Cm(^{48}Ca, xn)$^{296-x}$Lv [49]. A number of theoretical studies concentrating on the α-decay of ^{293}Lv have since been performed based on various models, including the relativistic [50, 51] and non-relativistic [50] mean-field models, the generalized liquid drop model [52], the Wigner–Kirkwood method [53], the two-center shell model [54], the cluster model [55–57], and the unified fission model [58]. Recently, similar to the previous JINR-FLNR experiment [49], the irradiation of ^{248}Cm targets with ^{48}Ca ions has been conducted [59] using the separator for heavy ion reaction products (SHIP) velocity filter at GSI in Darmstadt (Germany). In this experiment, the previously measured α-decay data were independently confirmed. Moreover, a new α-decay chain was observed, which was tentatively assigned to isomeric states. In fact, it has been shown that the existence and prevalence of long-lived isomers at low excitation energies in SHN enhances nuclear stability [60]. Moreover, in Ref. [61], it was pointed out that α-decay may not proceed through ground-state-to-ground-state chains, but rather through excited states. Therefore, it would be very interesting to investigate whether or not the newly observed α-decay chain in ^{293}Lv originates

from its isomeric state.

The covariant density functional theory (CDFT) has attracted widespread attention because of its considerable success in describing both the ground-state and excited-state properties of nuclei throughout the nuclide chart [62–66]. Recently, a new point-coupling density functional, PC-PK1, was proposed by fitting the masses, charge radii, and empirical pairing gaps of 60 selected spherical nuclei [67]. The powerful predictive ability of PC-PK1 has been illustrated through its descriptions of magnetic rotation [68], antimagnetic rotation [69, 70], low-lying exited states [65, 71, 72], and nuclear masses [73–75].

In this paper, two ^{293}Lv α-decay chains are investigated in the framework of CDFT with PC-PK1. Here, axial symmetry is assumed in the calculations, since the triaxiality and the reflection asymmetry are negligible in this region [76]. The pairing correlations are treated by the Bardeen–Cooper–Schrieffer (BCS) method with a density-independent zero-range force, where smooth cutoff is introduced to simulate the finite-range effects [77, 78]. Note that, since the nuclei under consideration in this study have odd neutron numbers, the unpaired neutron in each nucleus will block its occupied level in the BCS calculations, i.e., it will be prevented from participating in the nucleon pair scattering process due to the Pauli principle [79]. After blocking the possible single-particle levels (SPLs) near the Fermi surface, a series of nuclear states corresponding to different blocking levels will be obtained. The lowest-energy state is the ground state. Thus, in each iteration step of the CDFT calculation, one should ensure that the unpaired particle sits in the blocked SPL. A microscopic center-of-mass correction [80, 81] is adopted and the rotational correction is not considered. The Dirac equation for nucleons is solved in a harmonic oscillator basis using 20 major shells [82].

The potential energy curves (PECs) for the nuclei in the ^{293}Lv α-decay chains obtained by the adiabatic CDFT [83] are shown in Fig. 1. It can be seen that, for ^{293}Lv, two energy minima with total energies $E = -2082.45$ MeV and -2081.06 MeV undergoing prolate (quadrupole deformation, $\beta = 0.55$) and oblate ($\beta = -0.09$) deformations are obtained, which correspond to the ground state and the shape-isomeric state, respectively. Note that the isomeric state in ^{293}Lv is rather soft with respect to the β degree of freedom, although it has an energy that is approximately 1.39 MeV higher than its ground state. By following the ^{293}Lv α-decay chains, one can always find two energy minima at $\beta \sim 0.10$ and $\beta \sim 0.55$ for ^{289}Fl, ^{285}Cn, and ^{281}Ds. Further, in contrast to ^{293}Lv, their ground states have $\beta \sim 0.10$. With decreasing mass number A, the energy differences

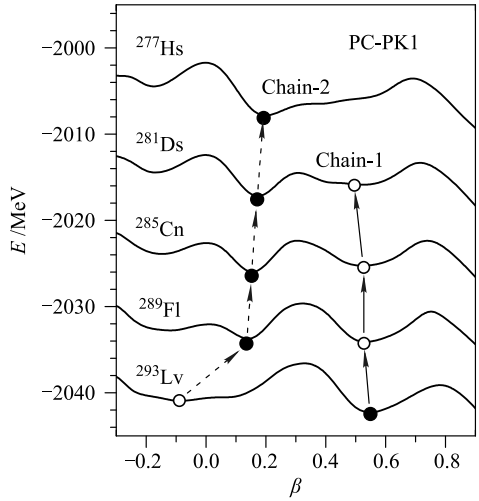

Fig. 1 The potential energy curves (PECs) for the nuclei in the ^{293}Lv α-decay chains obtained by the adiabatic covariant density functional theory with PC-PK1 [67]. For clarity, the PECs of Ds, Cn, Fl, and Lv are shifted upper respectively by 10, 20, 30, and 40 MeV. The solid and open circles denote ground states and shape-isomeric states, respectively. Two α-decay chains with similar deformations are connected with the solid and dashed arrows, respectively.

between the isomeric and ground states become increasingly large and, in the case of ^{277}Hs, the isomeric state at $\beta \sim 0.55$ finally disappears. Therefore, assuming similar deformations in the parent and daughter nuclei, one can clearly build two α-decay chains with similar deformations from the ground state (Chain-1) and shape-isomeric state (Chain-2) of ^{293}Lv. This assignment is consistent with experimental data [59], which shows that the two observed α-decay chains are terminated after three and four α decays through spontaneous fission. It should be noted that Chain-2 was tentatively assigned to high-spin isomers in Ref. [59], following analysis of the low-lying excited one-quasiparticle states using the Skyrme–Hartree–Fock–Bogoliubov method [84].

To understand the minima in the PECs in a microscopic manner, taking ^{293}Lv as an example, the proton and neutron SPLs near the Fermi surfaces as functions of β are shown in Fig. 2(a) and Fig. 2(b), respectively. For protons, it can be seen that two significant gaps occur near the Fermi surface at $\beta \sim -0.10$ and $\beta \sim 0.55$. For neutrons, a similar conclusion can also be drawn. Apparently, the two energy minima in the PEC of ^{293}Lv, as shown in Fig. 1, are connected to the two energy gaps observed in the SPLs.

Theoretically, by blocking each possible SPL near the Fermi surfaces, a series of E and β values corresponding to different blocking levels are obtained, which are tabulated in Table 1 and Table 2 for ^{293}Lv, ^{289}Fl, ^{285}Cn, ^{281}Ds, and ^{277}Hs at $\beta \sim 0.5$ for Chain-1 and $|\beta| \sim 0.1$ for Chain-2, respectively. The blocked levels are labeled

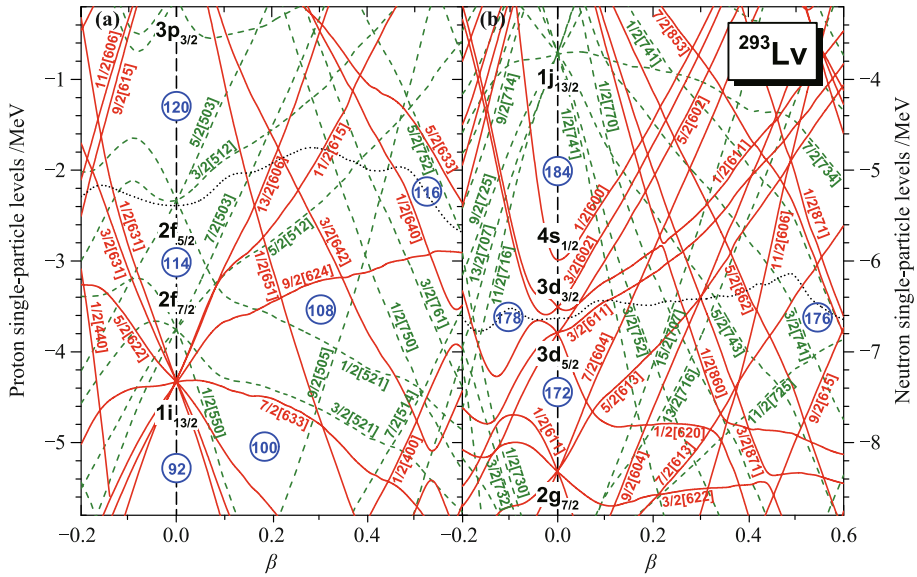

Fig. 2 **(a)** Proton and **(b)** neutron single-particle levels near the Fermi surfaces of ^{293}Lv as functions of the quadrupole deformation β. The positive and negative parity levels, whose major component is labeled by Nilsson numbers $\Omega[Nn_z\Lambda]$, are denoted by red solid and green dashed lines, respectively, and the Fermi surfaces are denoted by black dotted lines.

by the projection of the angular momentum on the symmetry axis Ω and parity π. To give a more intuitive picture, the E calculated by blocking different Ω^π levels for Chain-1 and Chain-2 are shown in Fig. 3 and Fig. 4, respectively, where the positive (negative) parity levels are represented by short solid (dashed) lines.

To facilitate a comparison with the experimental data for Chain-1 (Chain-2), eleven (ten) α-decay chains are theoretically built as follows:

(i) Assuming both the parent and daughter nuclei have the same Ω^π, for Chain-1 (Chain-2) eight (seven) α-decay chains are constructed, as shown in the rows in Table 1 (Table 2);

(ii) Assuming the parent and daughter nuclei are in the lowest-energy states regardless of their Ω^π, one α-decay chain can be constructed, which is represented by the black solid arrows in Fig. 3 (Fig. 4) for Chain-1 (Chain-2);

(iii) Assuming the parent and daughter nuclei are in the lowest-energy states with the same parity, two additional α-decay chains can be constructed, which are represented by the red dotted and green dashed arrows in Fig. 3 (Fig. 4) for Chain-1 (Chain-2).

For the first case, one can calculate the root mean square deviation ΔQ_α, as shown in the last column of Table 1 (Table 2) for Chain-1 (Chain-2), from

Table 1 By blocking each possible single-particle level Ω^π near the Fermi surfaces for the unpaired neutron, the calculated total energies E, quadrupole deformations β and Q_α values for Chain-1 in comparison with the data [59]. The lowest total energy for each nucleus is highlighted in boldface, and for each Ω^π, the root mean square deviation ΔQ_α defined in Eq. (1) is listed in the last column. All energies are expressed in MeV.

Chain-1	^{293}Lv			^{289}Fl			^{285}Cn			^{281}Ds		
Ω^π	E	β	Q_α	E	β	Q_α	E	β	Q_α	E	β	ΔQ_α
$1/2^-$	–2082.45	0.55	9.92	–2064.07	0.55	9.31	–2045.08	0.54	8.69	–2025.47	0.55	0.68
$3/2^-$	–2082.24	0.54	10.30	**–2064.24**	0.53	9.51	**–2045.45**	0.53	8.78	**–2025.93**	0.53	0.46
$5/2^-$	–2081.25	0.54	10.54	–2063.49	0.53	9.83	–2045.02	0.52	9.08	–2025.80	0.50	0.17
$11/2^-$	–2082.28	0.56	10.20	–2064.18	0.54	9.50	–2045.38	0.52	8.80	–2025.88	0.49	0.48
$1/2^+$	–2082.35	0.56	9.97	–2064.02	0.56	9.35	–2045.07	0.57	8.97	–2025.74	0.53	0.57
$5/2^+$	–2081.42	0.53	10.54	–2063.66	0.51	9.78	–2045.14	0.50	9.05	–2025.89	0.50	0.20
$7/2^+$	**–2082.49**	0.54	10.02	–2064.21	0.52	9.41	–2045.32	0.51	8.84	–2025.86	0.48	0.56
$9/2^+$	–2082.09	0.57	10.19	–2063.98	0.56	9.59	–2045.27	0.54	8.91	–2025.88	0.52	0.42
Exp.			10.68			9.96			9.31			

Table 2 Same as Table 1, but for Chain-2. The data are taken from Ref. [59].

Chain-2	^{293}Lv			^{289}Fl			^{285}Cn			^{281}Ds			^{277}Hs		
Ω^π	E	β	Q_α	E	β	Q_α	E	β	Q_α	E	β	Q_α	E	β	ΔQ_α
$13/2^-$	−2080.76	-0.12	9.92	−2062.38	0.15	11.07	−2045.15	0.16	10.06	−2026.91	0.18	9.24	−2007.85	0.20	0.60
$15/2^-$	−2080.11	0.13	12.47	**−2064.28**	0.13	10.01	−2045.99	0.14	9.07	−2026.76	0.16	8.60	−2007.06	0.18	1.08
$1/2^+$	**−2081.06**	-0.09	11.13	−2063.89	0.14	10.82	**−2046.41**	0.15	9.45	**−2027.56**	0.17	8.74	−2008.00	0.19	0.57
$3/2^+$	−2080.90	-0.09	11.06	−2063.66	0.14	10.83	−2046.19	0.15	9.61	−2027.50	0.17	8.91	**−2008.11**	0.19	0.49
$5/2^+$	−2080.66	-0.08	10.96	−2063.32	0.14	10.50	−2045.52	0.16	9.88	−2027.10	0.17	9.15	−2007.95	0.19	0.27
$7/2^+$	−2080.59	0.09	11.56	−2063.85	0.14	9.94	−2045.49	0.15	9.11	−2026.30	0.16	8.66	−2006.66	0.18	0.72
$9/2^+$	−2079.49	0.17	12.64	−2063.83	0.16	10.86	−2046.39	0.16	9.45	−2027.54	0.17	8.77	−2008.01	0.19	1.13
Exp.			10.65			10.17			9.85			9.45			

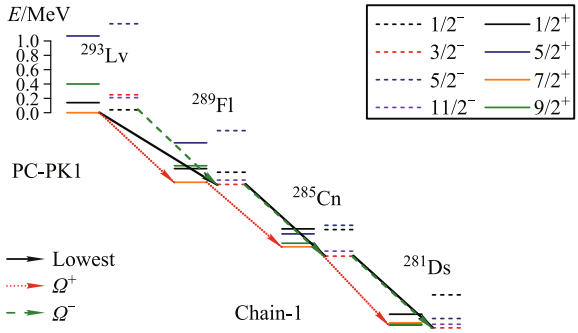

Fig. 3 The calculated total energies E for Chain-1 by blocking each possible single-particle level Ω^π near the Fermi surfaces for the unpaired neutron. The lowest-energy state for each nucleus and those with the positive and negative parity are connected with black solid, red dotted, and green dashed arrows, respectively.

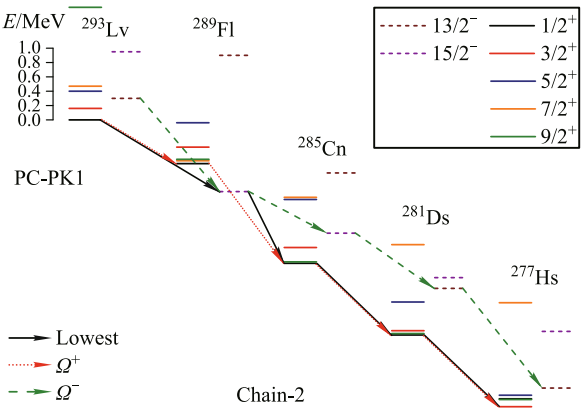

Fig. 4 Same as Fig. 3, but for Chain-2.

$$\Delta Q_\alpha = \sqrt{\sum_{i=1}^{N-1}\left(Q_{\alpha_i}^{\mathrm{Cal.}} - Q_{\alpha_i}^{\mathrm{Exp.}}\right)^2/(N-1)}\,, \qquad (1)$$

where N is the number of nuclei involved in a given α-decay chain. It can be seen that the α-decay chain with $5/2^-$ can best reproduce the data for Chain-1, while $5/2^+$ yields the optimum agreement with the Chain-2 data.

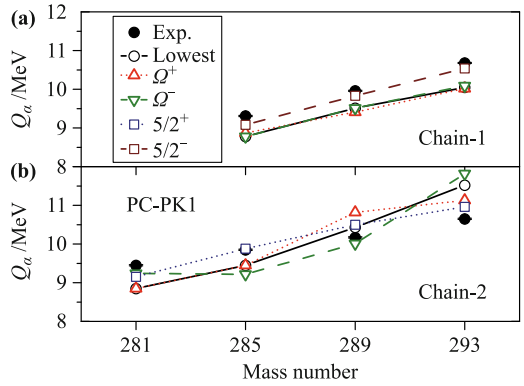

Fig. 5 The calculated Q_α values for Chain-1 **(a)** and Chain-2 **(b)** of the α-decay chains built on $5/2^+$ or $5/2^-$ state (*open squares*) and the lowest-energy state with (*open triangles*) and without (*open circles*) the same parity for each nucleus in comparison with the data [59].

For the latter two cases, where the emitted α particle has a nonzero angular momentum due to the different Ω^π values of the parent and daughter nuclei (meaning that this α-decay is quenched by the centrifugal barrier), the calculated Q_α values are compared with the data in Figs. 5(a) and (b) for Chain-1 and Chain-2, respectively. One can see that it was possible for the experimental data for both α-decay chains to be well reproduced within 1 MeV. However, it is difficult to determine whether or not the parity is changed in the present mean-field framework.

An accurate description of the Q_α value is related to the description of the total energies for the parent and daughter nuclei. Previous systematic investigation has revealed that, although the accuracy for nuclear mass is approximately 2.3 MeV, the accuracy for one-neutron separation energy is approximately 0.6 MeV [85]. For the density functional PC-PK1, the accuracy for nuclear mass is improved to 1.4 MeV [66]. The accuracy for one-neutron separation energy and the Q_α value should, therefore, be improved accordingly.

In summary, in this paper, ^{293}Lv α-decay chains are investigated in the framework of covariant density func-

tional theory with PC-PK1, where the pairing correlations are treated by the Bardeen-Cooper-Schrieffer method with a density-independent zero-range force. From the obtained potential energy curves, it is found that the two α-decay chains observed in ^{293}Lv may originate from the ground state (Chain-1) and the shape-isomeric state (Chain-2) of ^{293}Lv. By assuming that both the parent and daughter nuclei have the same Ω^{π}, the experimental Q_{α} values for Chain-1 and Chain-2 can be reproduced quite well by the two α-decay chains built on $5/2^{-}$ and $5/2^{+}$, respectively. Further, by assuming that both the parent and daughter nuclei are in the lowest-energy states, the experimental data can be reproduced with the same accuracy regardless of whether or not the parity is changed. Finally, it may be possible to distinguish between these α-decay chains by further comparing the resultant α-decay half-lives, which depend not only on the Q_{α} value, but also on the angular momentum of the emitted α particle.

Acknowledgements The authors are indebted to S. Heinz, J. Meng, and S. Q. Zhang for their valuable suggestions and critical reviews. This work was supported by the Major State 973 Program of China (Grant No. 2013CB834400), the National Natural Science Foundation of China (Grant Nos. 11005004, 11175002, 11275098, and 11335002), the Research Fund for the Doctoral Program of Higher Education (Grant No. 20110001110087), and the China Postdoctoral Science Foundation (Grant Nos. 2012M520101 and 2013M540011).

References

1. W. D. Myers and W. J. Swiatecki, Nuclear masses and deformations, *Nucl. Phys.* 81(2), 1 (1966)
2. A. Sobiczewski, F. A. Gareev, and B. N. Kalinkin, Closed shells for $Z > 82$ and $N > 126$ in a diffuse potential well, *Phys. Lett.* 22(4), 500 (1966)
3. H. Meldner, Predictions of new magic regions and masses for super-heavy nuclei from calculations with realistic shell model single particle Hamiltonians, *Ark. Fys.* 36, 593 (1967)
4. S. G. Nilsson, J. R. Nix, A. Sobiczewski, Z. Szymański, S. Wycech, C. Gustafson, and P. Möller, On the spontaneous fission of nuclei with Z near 114 and N near 184, *Nucl.Phys. A* 115(3), 545 (1968)
5. S. G. Nilsson, C. F. Tsang, A. Sobiczewski, Z. Szymański, S. Wycech, C. Gustafson, I. L. Lamm, P. Möller, and B. Nilsson, On the nuclear structure and stability of heavy and superheavy elements, *Nucl. Phys. A* 131(1), 1 (1969)
6. S. G. Nilsson, S. G. Thompson, and C. F. Tsang, Stability of superheavy nuclei and their possible occurrence in nature, *Phys. Lett. B* 28(7), 458 (1969)
7. U. Mosel and W. Greiner, On the stability of superheavy nuclei against fission, *Z. Phys.* 222(3), 261 (1969)
8. J. Grumann, U. Mosel, B. Fink, and W. Greiner, Investigation of the stability of superheavy nuclei around $Z = 114$ and $Z = 164$, *Z. Phys.* 228(5), 371 (1969)
9. S. Hofmann and G. Münzenberg, The discovery of the heaviest elements, *Rev. Mod. Phys.* 72(3), 733 (2000)
10. Yu. Ts. Oganessian, Heaviest nuclei from ^{48}Ca-induced reactions, *J. Phys. G* 34(4), R165 (2007)
11. Yu. Ts. Oganessian, F. Sh. Abdullin, P. D. Bailey, D. E. Benker, M. E. Bennett, S. N. Dmitriev, J. G. Ezold, J. H. Hamilton, R. A. Henderson, M. G. Itkis, Yu. V. Lobanov, A. N. Mezentsev, K. J. Moody, S. L. Nelson, A. N. Polyakov, C. E. Porter, A. V. Ramayya, F. D. Riley, J. B. Roberto, M. A. Ryabinin, K. P. Rykaczewski, R. N. Sagaidak, D. A. Shaughnessy, I. V. Shirokovsky, M. A. Stoyer, V. G. Subbotin, R. Sudowe, A. M. Sukhov, Yu. S. Tsyganov, V. K. Utyonkov, A. A. Voinov, G. K. Vostokin, and P. A. Wilk, Synthesis of a new element with atomic number $Z = 117$, *Phys. Rev. Lett.* 104(14), 142502 (2010)
12. K. Morita, K. Morimoto, D. Kaji, T. Akiyama, S. I. Goto, H. Haba, E. Ideguchi, R. Kanungo, K. Katori, H. Koura, H. Kudo, T. Ohnishi, A. Ozawa, T. Suda, K. Sueki, H. S. Xu, T. Yamaguchi, A. Yoneda, A. Yoshida, and Y. L. Zhao, Experiment on the synthesis of element 113 in the reaction ^{209}Bi(^{70}Zn, n)^{278}113, *J. Phys. Soc. Jpn.* 73(10), 2593 (2004)
13. K. Morita, K. Morimoto, D. Kaji, T. Akiyama, S. I. Goto, H. Haba, E. Ideguchi, K. Katori, H. Koura, H. Kikunaga, H. Kudo, T. Ohnishi, A. Ozawa, N. Sato, T. Suda, K. Sueki, F. Tokanai, T. Yamaguchi, A. Yoneda, and A. Yoshida, Observation of second decay chain from ^{278}113, *J. Phys. Soc. Jpn.* 76(4), 045001 (2007)
14. A. Sobiczewski and K. Pomorski, Description of structure and properties of superheavy nuclei, *Prog. Part. Nucl. Phys.* 58(1), 292 (2007)
15. M. Bender, P. H. Heenen, and P. G. Reinhard, Selfconsistent mean-field models for nuclear structure, *Rev. Mod. Phys.* 75(1), 121 (2003)
16. G. A. Lalazissis, M. M. Sharma, P. Ring, and Y. K. Gambhir, Superheavy nuclei in the relativistic mean-field theory, *Nucl. Phys. A* 608(2), 202 (1996)
17. J. Meng and N. Takigawa, Structure of superheavy elements suggested in the reaction of ^{86}Kr with ^{208}Pb, *Phys. Rev. C* 61(6), 064319 (2000)
18. Z. Z. Ren and H. Toki, Superdeformation in the newly discovered superheavy elements, *Nucl. Phys. A* 689(3–4), 691 (2001)
19. M. Bender, K. Rutz, P. G. Reinhard, J. A. Maruhn, and W. Greiner, Shell structure of superheavy nuclei in self-consistent mean-field models, *Phys. Rev. C* 60(3), 034304 (1999)
20. A. T. Kruppa, M. Bender, W. Nazarewicz, P. G. Reinhard, T. Vertse, and S. Ćwiok, Shell corrections of superheavy nuclei in self-consistent calculations, *Phys. Rev. C* 61(3), 034313 (2000)

21. W. Zhang, S. S. Zhang, S. Q. Zhang, and J. Meng, Shell correction at the saddle point for superheavy nucleus, *Chin. Phys. Lett.* 20(10), 1694 (2003)
22. W. Zhang, J. Meng, S. Q. Zhang, L. S. Geng, and H. Toki, Magic numbers for superheavy nuclei in relativistic continuum Hartree–Bogoliubov theory, *Nucl. Phys. A* 753(1–2), 106 (2005)
23. W. H. Long, J. Meng, and S. G. Zhou, Structure of the new nuclide ^{259}Db and its α-decay daughter nuclei, *Phys. Rev. C* 65(4), 047306 (2002)
24. L. S. Geng, H. Toki, and J. Meng, α-decay chains of $^{288}_{173}115$ and $^{287}_{172}115$ in the relativistic mean field theory, *Phys. Rev. C* 68, 061303(R) (2003)
25. T. Bürvenich, M. Bender, J. A. Maruhn, and P. G. Reinhard, Systematics of fission barriers in superheavy elements, *Phys. Rev. C* 69(1), 014307 (2004)
26. Z. P. Li, T. Nikšić, D. Vretenar, P. Ring, and J. Meng, Relativistic energy density functionals: Low-energy collective states of ^{240}Pu and ^{166}Er, *Phys. Rev. C* 81(6), 064321 (2010)
27. B. N. Lu, E. G. Zhao, and S. G. Zhou, Potential energy surfaces of actinide nuclei from a multidimensional constrained covariant density functional theory: Barrier heights and saddle point shapes, *Phys. Rev. C* 85(1), 011301(R) (2012)
28. H. Abusara, A. V. Afanasjev, and P. Ring, Fission barriers in covariant density functional theory: Extrapolation to superheavy nuclei, *Phys. Rev. C* 85(2), 024314 (2012)
29. M. Warda and J. L. Egido, Fission half-lives of superheavy nuclei in a microscopic approach, *Phys. Rev. C* 86(1), 014322 (2012)
30. V. Prassa, T. Nikšić, G. A. Lalazissis, and D. Vretenar, Relativistic energy density functional description of shape transitions in superheavy nuclei, *Phys. Rev. C* 86(2), 024317 (2012)
31. G. G. Adamian, N. V. Antonenko, W. Scheid, and V. V. Volkov, Fusion cross sections for superheavy nuclei in the dinuclear system concept, *Nucl. Phys. A* 633(3), 409 (1998)
32. Z. Q. Feng, G. M. Jin, J. Q. Li, and W. Scheid, Formation of superheavy nuclei in cold fusion reactions, *Phys. Rev. C* 76(4), 044606 (2007)
33. E. G. Zhao, N. Wang, Z. Q. Feng, J. Q. Li, S. G. Zhou, and W. Scheid, The isotopic and nuclear orientation effects on the production of super-heavy elements, *Int. J. Mod. Phys. E* 17(09), 1937 (2008)
34. A. K. Nasirov, G. Giardina, G. Mandaglio, M. Manganaro, F. Hanappe, S. Heinz, S. Hofmann, A. I. Muminov, and W. Scheid, Quasifission and fusion-fission in reactions with massive nuclei: Comparison of reactions leading to the $Z = 120$ element, *Phys. Rev. C* 79(2), 024606 (2009)
35. J. Q. Li, Z. Q. Feng, Z. G. Gan, X. H. Zhou, H. F. Zhang, and W. Scheid, Production of superheavy nuclei in massive fusion reactions, *Nucl. Phys. A* 834(1–4), 353c (2010)
36. Z. Q. Feng, G. M. Jin, and J. Q. Li, Dynamics in production of superheavy nuclei in low-energy heavy-ion collision, *Nucl. Phys. Rev.* 28, 1 (2011)
37. N. Wang, E. G. Zhao, W. Scheid, and S. G. Zhou, Theoretical study of the synthesis of superheavy nuclei with $Z = 119$ and 120 in heavy-ion reactions with transuranium targets, *Phys. Rev. C* 85(4), 041601(R) (2012)
38. Y. Aritomo, T. Wada, M. Ohta, and Y. Abe, Fluctuation dissipation model for synthesis of superheavy elements, *Phys. Rev. C* 59(2), 796 (1999)
39. J. D. Bao and Y. Z. Zhuo, Investigation on anomalous diffusion for nuclear fusion reactions, *Phys. Rev. C* 67(6), 064606 (2003)
40. W. J. Świątecki, K. Siwek-Wilczyńska, and J. Wilczyński, Fusion by diffusion (II): Synthesis of transfermium elements in cold fusion reactions, *Phys. Rev. C* 71(1), 014602 (2005)
41. Z. H. Liu and J. D. Bao, Optimal reaction for synthesis of superheavy element 117, *Phys. Rev. C* 80(3), 034601 (2009)
42. K. Siwek-Wilczyńska, T. Cap, M. Kowal, A. Sobiczewski, and J. Wilczyński, Predictions of the fusion-by-diffusion model for the synthesis cross sections of $Z = 114$–120 elements based on macroscopic-microscopic fission barriers, *Phys. Rev. C* 86(1), 014611 (2012)
43. N. Wang, X. Z. Wu, Z. X. Li, M. Liu, and W. Scheid, Applications of Skyrme energy-density functional to fusion reactions for synthesis of superheavy nuclei, *Phys. Rev. C* 74(4), 044604 (2006)
44. B. A. Bian, F. S. Zhang, and H. Y. Zhou, Entrance channel mass asymmetry dependence of compound nucleus formation, *Phys. Lett. B* 665(4), 314 (2008)
45. C. W. Shen, G. Kosenko, and Y. Abe, Two-step model of fusion for the synthesis of superheavy elements, *Phys. Rev. C* 66(6), 061602(R) (2002)
46. V. I. Zagrebaev, Synthesis of superheavy nuclei: Nucleon collectivization as a mechanism for compound nucleus formation, *Phys. Rev. C* 64(3), 034606 (2001)
47. V. I. Zagrebaev and W. Greiner, Synthesis of superheavy nuclei: A search for new production reactions, *Phys. Rev. C* 78(3), 034610 (2008)
48. Yu. Ts. Oganessian, V. K. Utyonkov, Yu. V. Lobanov, F. Sh. Abdullin, A. N. Polyakov, I. V. Shirokovsky, Yu. S. Tsyganov, G. G. Gulbekian, S. L. Bogomolov, B. N. Gikal, A. N. Mezentsev, S. Iliev, V. G. Subbotin, A. M. Sukhov, A. A. Voinov, G. V. Buklanov, K. Subotic, V. I. Zagrebaev, M. G. Itkis, J. B. Patin, K. J. Moody, J. F. Wild, M. A. Stoyer, N. J. Stoyer, D. A. Shaughnessy, J. M. Kenneally, and R. W. Lougheed, Measurements of cross sections for the fusion-evaporation reactions ^{244}Pu(^{48}Ca,xn)$^{292-x}$114 and ^{245}Cm(^{48}Ca,xn)$^{293-x}$116, *Phys. Rev. C* 69(5), 054607 (2004)
49. Yu. Ts. Oganessian, V. K. Utyonkov, Yu. V. Lobanov, F. Sh. Abdullin, A. N. Polyakov, I. V. Shirokovsky, Yu. S. Tsyganov, G. G. Gulbekian, S. L. Bogomolov, B. N. Gikal, A. N. Mezentsev, S. Iliev, V. G. Subbotin, A. M. Sukhov, A. A. Voinov, G. V. Buklanov, K. Subotic, V. I. Zagrebaev, M. G. Itkis, J. B. Patin, K. J. Moody, J. F. Wild, M. A. Stoyer, N. J. Stoyer, D. A. Shaughnessy, J. M. Kenneally, P.

A. Wilk, R. W. Lougheed, R. I. Il'kaev, and S. P. Vesnovskii, Measurements of cross sections and decay properties of the isotopes of elements 112, 114, and 116 produced in the fusion reactions ^{233,238}U, ^{242}Pu, and ^{248}Cm+^{48}Ca, *Phys. Rev. C* 70, 064609 (2004)

50. S. K. Singh, M. Ikram, and S. K. Patra, Ground state properties and bubble structure of synthesized superheavy nuclei, *Int. J. Mod. Phys. E* 22(01), 1350001 (2013)
51. M. Bhattacharya and G. Gangopadhyay, α-decay lifetime in superheavy nuclei with $A > 282$, *Phys. Rev. C* 77(4), 047302 (2008)
52. H. F. Zhang, W. Zuo, J. Q. Li, and G. Royer, α decay half-lives of new superheavy nuclei within a generalized liquid drop model, *Phys. Rev. C* 74(1), 017304 (2006)
53. A. Bhagwat, X. Viñas, M. Centelles, P. Schuck, and R. Wyss, Microscopic-macroscopic approach for binding energies with the Wigner–Kirkwood method (II): Deformed nuclei, *Phys. Rev. C* 86(4), 044316 (2012)
54. A. N. Kuzmina, G. G. Adamian, and N. V. Antonenko, Role of quasiparticle structure in α decays of the heaviest nuclei, *Phys. Rev. C* 85(2), 027308 (2012)
55. Y. B. Qian, Z. Z. Ren, and D. D. Ni, Calculations of α-decay half-lives for heavy and superheavy nuclei, *Phys. Rev. C* 83(4), 044317 (2011)
56. D. D. Ni and Z. Z. Ren, Microscopic calculation of α-decay half-lives within the cluster model, *Nucl. Phys. A* 825(3–4), 145 (2009)
57. D. D. Ni and Z. Z. Ren, Calculations of new α-decay data within the generalized density-dependent cluster model, *J. Phys. G* 37(10), 105107 (2010)
58. J. M. Dong, W. Zuo, J. Z. Gu, Y. Z. Wang, and B. B. Peng, α-decay half-lives and Q_α values of superheavy nuclei, *Phys. Rev. C* 81(6), 064309 (2010)
59. S. Hofmann, S. Heinz, R. Mann, J. Maurer, J. Khuyagbaatar, D. Ackermann, S. Antalic, W. Barth, M. Block, H. G. Burkhard, V. F. Comas, L. Dahl, K. Eberhardt, J. Gostic, R. A. Henderson, J. A. Heredia, F. P. Heßberger, J. M. Kenneally, B. Kindler, I. Kojouharov, J. V. Kratz, R. Lang, M. Leino, B. Lommel, K. J. Moody, G. Münzenberg, S. L. Nelson, K. Nishio, A. G. Popeko, J. Runke, S. Saro, D. A. Shaughnessy, M. A. Stoyer, P. Thörle-Pospiech, K. Tinschert, N. Trautmann, J. Uusitalo, P. A. Wilk, and A. V. Yeremin, The reaction ^{48}Ca + ^{248}Cm→ ^{296}116* studied at the GSI-SHIP, *Eur. Phys. J. A* 48(5), 62 (2012)
60. F. R. Xu, E. G. Zhao, R. Wyss, and P. M. Walker, Enhanced stability of superheavy nuclei due to high-spin isomerism, *Phys. Rev. Lett.* 92(25), 252501 (2004)
61. D. S. Delion, R. J. Liotta, and R. Wyss, α decay of highspin isomers in superheavy nuclei, *Phys. Rev. C* 76(4), 044301 (2007)
62. P. Ring, Relativistic mean field theory in finite nuclei, *Prog. Part. Nucl. Phys.* 37, 193 (1996)
63. D. Vretenar, A. V. Afanasjev, G. A. Lalazissis, and P. Ring, Relativistic Hartree–Bogoliubov theory: Static and dynamic aspects of exotic nuclear structure, *Phys. Rep.* 409(3–4), 101 (2005)
64. J. Meng, H. Toki, S. G. Zhou, S. Q. Zhang, W. H. Long, and L. S. Geng, Relativistic continuum Hartree Bogoliubov theory for ground-state properties of exotic nuclei, *Prog. Part. Nucl. Phys.* 57(2), 470 (2006)
65. T. Nikšić, D. Vretenar, and P. Ring, Relativistic nuclear energy density functionals: Mean-field and beyond, *Prog. Part. Nucl. Phys.* 66(3), 519 (2011)
66. J. Meng, J. Peng, S. Q. Zhang, and P. W. Zhao, Progress on tilted axis cranking covariant density functional theory for nuclear magnetic and antimagnetic rotation, *Front. Phys.* 8(1), 55 (2013)
67. P. W. Zhao, Z. P. Li, J. M. Yao, and J. Meng, New parametrization for the nuclear covariant energy density functional with a point-coupling interaction, *Phys. Rev. C* 82(5), 054319 (2010)
68. P. W. Zhao, S. Q. Zhang, J. Peng, H. Z. Liang, P. Ring, and J. Meng, Novel structure for magnetic rotation bands in ^{60}Ni, *Phys. Lett. B* 699(3), 181 (2011)
69. P. W. Zhao, J. Peng, H. Z. Liang, P. Ring, and J. Meng, Antimagnetic rotation band in nuclei: A microscopic description, *Phys. Rev. Lett.* 107(12), 122501 (2011)
70. P. W. Zhao, J. Peng, H. Z. Liang, P. Ring, and J. Meng, Covariant density functional theory for antimagnetic rotation, *Phys. Rev. C* 85(5), 054310 (2012)
71. J. M. Yao, J. Meng, P. Ring, Z. X. Li, Z. P. Li, and K. Hagino, Microscopic description of quantum shape fluctuation in C isotopes, *Phys. Rev. C* 84(2), 024306 (2011)
72. Z. P. Li, C. Y. Li, J. Xiang, J. M. Yao, and J. Meng, Enhanced collectivity in neutron-deficient Sn isotopes in energy functional based collective Hamiltonian, *Phys. Lett. B* 717(4–5), 470 (2012)
73. B. H. Sun, P. W. Zhao, and J. Meng, Mass prediction of proton-rich nuclides with the Coulomb displacement energies in the relativistic point-coupling model, *Sci. China Ser. G* 54, 210 (2011)
74. P. W. Zhao, L. S. Song, B. H. Sun, H. Geissel, and J. Meng, Crucial test for covariant density functional theory with new and accurate mass measurements from Sn to Pa, *Phys. Rev. C* 86(6), 064324 (2012)
75. Q. S. Zhang, Z. M. Niu, Z. P. Li, J. M. Yao, and J. Meng, Global dynamical correlation energies in covariant density functional theory: Cranking approximation, *Front. Phys.* 9(4), 529 (2014)
76. W. Zhang, Z. P. Li, and S. Q. Zhang, Description of α-decay chains for ^{293,294}117 within covariant density functional theory, *Phys. Rev. C* 88(5), 054324 (2013)
77. S. J. Krieger, P. Bonche, H. Flocard, P. Quentin, and M. S. Weiss, An improved pairing interaction for mean field calculations using Skyrme potentials, *Nucl. Phys. A* 517(2), 275 (1990)

78. M. Bender, K. Rutz, P. G. Reinhard, and J. A. Maruhn, Pairing gaps from nuclear mean-field models, *Eur. Phys. J. A* 8(1), 59 (2000)
79. P. Ring and P. Schuck, The Nuclear Many-Body Problem, Berlin: Springer-Verlag, 1980
80. M. Bender, K. Rutz, P. G. Reinhard, and J. A. Maruhn, Consequences of the center-of-mass correction in nuclear mean-field models, *Eur. Phys. J. A* 7(4), 467 (2000)
81. P. W. Zhao, B. Y. Sun, and J. Meng, Deformation effect on the center-of-mass correction energy in nuclei ranging from Oxygen to Calcium, *Chin. Phys. Lett.* 26(11), 112102 (2009)
82. P. Ring, Y. K. Gambhir, and G. A. Lalazissis, Computer program for the relativistic mean field description of the ground state properties of even-even axially deformed nuclei, *Comput. Phys. Commun.* 105(1), 77 (1997)
83. J. Meng, J. Peng, S. Q. Zhang, and S. G. Zhou, Possible existence of multiple chiral doublets in ^{106}Rh, *Phys. Rev. C* 73(3), 037303 (2006)
84. S. Ćwiok, W. Nazarewicz, and P. H. Heenen, Structure of odd-N superheavy elements, *Phys. Rev. Lett.* 83(6), 1108 (1999)
85. L. S. Geng, H. Toki, and J. Meng, Masses, deformations and charge radii—Nuclear ground-state properties in the relativistic mean field model, *Prog. Theor. Phys.* 113(4), 785 (2005)